MINIMUM BREAKDOWN VOLTAGES FOR CORONA DISCHARGE IN CYLINDRICAL AND SPHERICAL GEOMETRIES

Aaron S. Gibson*, Jeremy A. Riousset†, and Victor P. Pasko‡

CSSL Department of Electrical Engineering
The Pennsylvania State University, University Park, PA 16802

*Undergraduate student of
Electrical and Computer Engineering
University of Arizona
Tucson, AZ 85719

ABSTRACT

The lightning rod was invented in the mid-1700's by Benjamin Franklin, who suggested that the rods should have sharp tips to increase the concentration of electric fields, and also to prevent the rod from rusting.[1, 2] More recently, Moore *et al.* suggested that the strike-reception probabilities of Benjamin Franklin's rods are greatly increased when their tips are made moderately blunt.[2] In this work, we use Townsend's equation for corona discharge, to find a critical radius and minimum breakdown voltage for cylindrical and spherical geometries. We solve numerically the system of equations and present simple analytical formulas for the aforementioned geometies. These formulas complement the classic theory developed in the framework of Townsend theory.[3, 4]

INTRODUCTION

Interest in lightning protection has been renewed in the past decades due to potential hazards to a variety of modern systems, such as buildings, electric power and communications systems, electronic integrated circuit chips, aircraft, and boats.[5] Current lightning protection devices can reduce damage in two different ways: (1)

†Graduate Mentor
‡Faculty Mentor

by hampering the formation of lightning, (2) by intercepting the lightning through a lightning rod.[6, 7] Understanding the complex nature of lightning is made challenging by the difficulty of reproducing atmospheric processes in laboratories. These difficulties are accentuated by the many scales of the lightning phenomenon, which involves microphysical processes developing in a multi-kilometer scale discharge.[7] However, it is now understood that lightning is an atmospheric discharge of the same nature as the spark.[3]

ELECTRON AVALANCHES, CORONA, STREAMERS, AND LEADERS

The building block of any electrical discharge is the electron avalanche.[3] The avalanche begins with a small number of "seed" electrons that appear accidentally, for example due to cosmic rays.[3] Under the influence of an electric field, these electrons gain kinetic energy which is lost in collisions with neutral particles,[8] ionizing these particles and creating new electrons. The so-created electrons experience the same acceleration as the seed electrons, until they collide with more atoms creating new ions and electrons[3, 9]. The process repeats itself forming the "electron avalanche."

A glow corona can be observed in the dark or in bad weather on high-power transmission lines or as St. Elmo's fires on the mast of a ship or airplane.[5] Glow coronae are also responsible in part for the noise of a transistor radio.[5, 9] Physically, a glow corona developing near a grounded object under severe weather conditions is a region of moderately ionized plasma that conducts a very small ionic current, on the order of a few μA, though approaching lightning can cause the current to increase to a few mA.[10] The electric field around the tip of a lightning rod will vary with geometry, but it can hypothetically range from 0.2 kV/cm to 2.7 kV/cm depending on the proximity (or existence thereof) of an approaching lightning.[10]

Glow coronae are formed in strongly nonuniform electric fields[3] by ionization of the neutral particles of air. In order to maintain the corona discharge, the electrons released during the ionization process must replace the electrons lost to attachment to ambient molecules.[3] The rate of ionization is therefore fundamental and is expressed as the ionization coefficient, α, which measures the number of ionization events performed by an electron in a 1 cm path along the electric field.[3] Each electron has an exponential effect towards the avalanche, which can be described by the following equation:[3, 4, 11]

$$\int_{R_1}^{R_2} \alpha \, dr = \ln Q \tag{1}$$

where Q is the number of electrons in the avalanche, R_1 and R_2 are the positions of the first and second electrode respectively, $d = R_2 - R_1$ is the distance between the two electrodes and r is the position between the electrodes. The value, $Q = 10^4$, is used in this paper, since this value is in good agreement with published experimental values for point and wire configurations, and also for positive and negative corona.[11]

In the case of atmospheric discharges, glow corona can greatly influence the initiation of more ionized plasma discharges such as streamers and leaders, discussed hereafter.[10] Streamers are moderately, one can even say weakly ionized plasma channels that are necessary for the extension of leader channels, constituting the lightning branches.[3] In the case of atmospheric discharges, streamers are produced and destroyed at the rate of $\sim 10^9$ Hz[12] in the so-called streamer zone of the atmospheric lightning channel. Streamers can be self-sustained[13] and propagate due to the relatively high electric field at their tip also referred to as the streamer head.[14]

Streamers can lead to perhaps the most notorious atmospheric discharge: lightning. The lightning channel is commonly called a leader.[9] Leaders are highly conductive plasma filaments,[3] with very high ionization currents, on the order of several kA.[5] Bazelyan and Raizer[9] stated that the foremost condition of leader formation in air is an increase in gas temperature, at least to the extent necessary to suppress a decrease in conductivity owing to electron attachment.[9] The temperature of a leader is $\gtrsim$ 5000 K, which is significantly higher than the 300 K typical of streamer corona.[14, 15] This increase in temperature is due to the merging of the streamer currents starting from the leader tip.[16] An increase in conductivity due to an increase in temperature will result in the narrowing of current flow to a thin channel.[9] The currents of all of the streamers starting from a leader tip are summed up, leading to Joule heating of the region ahead of the tip and therefore to increase in its thermal energy.[14] The increase in thermal energy will increase the conductivity of the region ahead of the tip, thus extending the channel further. The process of leader propagation is not fully understood[17] at present and falls beyond the scope of this present paper. A brief summary comparing the types of discharges discussed previously is given in Table I.

Table I: Atmospheric discharge characteristics at ground level (adapted from [14]).

Parameter	Glow Corona	Streamer	Leader
Temperature	$\sim$300 K	$\sim$300 K[14]	$\gtrsim$ 5000 K[9, 15]
Electron energy	1–2 eV[4]	5–15 eV[15]	1–2 eV[18]
Electric field	0.2–2.7 kV/cm[10]	5–7.5 kV/cm[15]	1–5 kV/cm[9]
Electron density	2.6×10^8 cm^{-3}[3]	5×10^{13}–10^{15}cm^{-3}[9, 15]	4×10^{14}cm^{-3}[13]

TOWNSEND BREAKDOWN

Townsend's model deals with dark discharge and glow corona (the primary difference between the two being the luminous "glow"). Townsend discharge occurs in the presence of two parallel plate electrodes with a voltage difference of a few kV in standard conditions in between them. Based on experimental data, Townsend suggested a formula for the ionization coefficient, α:[3, 19]

$$\alpha = Ape^{-\frac{Bp}{E}} \tag{2}$$

where A (1/cm/Torr) and B (V/cm/Torr) are empirically calculated constants that vary with the composition of the gas, p is pressure of the gas in Torr, and E is the electric field in V/cm.[3, 4] Using equations (1) and (2) and Poisson's equation, a critical (minimum) breakdown voltage can be derived and plotted as graphs known as the Paschen curves.[3] Of particular interest in this paper is Stoletov's point, which is the point of maximum current and more importantly minimum voltage for the initiation of corona discharge in a plane-plane configuration.[4]

It is believed that corona discharge may attract approaching downward leaders[20–22]. Based on repeated observation, it is generally accepted that a lightning leader progresses to about 10 m above the ground until the electric field at a point on the ground surface has increased sufficiently to cause an upward leader to be initiated.[23] The upward-leader evolves from a corona discharge into a high current leader, which can establish a connecting path with the downward lightning leader.[20] Since this observation holds if the object struck is fitted with a lightning rod,[21] an ideal lightning rod should readily produce an upward connecting leader.

In the application of lightning rods, experimental results suggest that lightning rods with blunt tips are more effective than the rods with sharp tips.[1, 2, 24, 25] The effectiveness of the blunt-tipped rod is suggested to be related to the corona onset on the geometry of the rod.[11] To date, a full quantitative description of upward leader development is yet to be developed. A simple first-order approximation of the corona discharge is needed, because the effect it has on the leader initiation and therefore on a lightning protection device's efficiency is not negligible.[26] The conversion of corona into an upward leader is a critical part of the lightning attachment process.[22] Lowke and D'Alessandro[11, 25] formulated theoretical models of glow corona around the lightning rod tip using variations of Peek's formula ($E_c = 30\delta\left(1 + \frac{0.3}{\sqrt{\delta R_1}}\right)$, where E_c is in kV/cm and δ is the relative air density[11]). However, Peek's formula does not allow for the evaluation of the minimum breakdown voltage as a function of the rod's radius. Gary *et al.*[19] suggested the use of $\alpha = k\frac{p}{p_0}\left(\left(\frac{E}{E_0}\right)^2\left(\frac{p_0}{p}\right)^2 - 1\right)$ instead of Townsend's equation (2), where p_0 is a reference pressure ($\approx 10^5$ Pa) and E_0 is the reference electric field ($\approx$ 24-31 kV/cm) at p_0. Gary *et al.*[19] state that Townsend's law is satisfactory for higher values of $\frac{E}{p}$, but dismisses the use of Townsend's equation for lower values.[19] Lowke and D'Alessandro[11] theorized that the Townsend mechanism would suggest that results are dependent on electrode materials. However, the experimental results are remarkably independent of the composition of the electrodes.[11] On the other hand, the use of Townsend's breakdown criterion allows for the estimation of the minimum breakdown voltage.

In this work, the constants A and B are fitted to an exact formulation for α[8]:

$$\alpha = \frac{\nu_i(E) - \nu_{a_2}(E)}{\mu_e(E)E}$$

where ν_i, ν_{a_2}, and μ_e are the ionization frequency, two body attachment frequency, and electron mobility respectively. ν_i, ν_{a_2}, and μ_i are obtained using models formulated by Morrow and Lowke[27]. The coefficients A and B are calculated using an exponential fit to the curve $\frac{E}{N}$ vs. $\frac{\alpha}{N}$, where N is the atmospheric neutral density. In this work, the electric field and minimum breakdown voltage for the initiation of the corona surrounding a lightning rod are calculated numerically and approximated analytically for the cases of cylindrical and spherical geometries.

MODEL FORMULATION

In equation (2), A and B are dependent on the composition of the gas. Raizer[3] uses values of $A = 15$ 1/cm/Torr and $B = 365$ V/cm/Torr; however, better approximations can be obtained based on the numerical results of Morrow and Lowke§.[27] Using an exponential fit with values of α obtained using these results[27] for ν_i, ν_{a_2}, and μ_e, the optimal values are: $A = 7.0$ 1/cm/Torr and $B = 258$ V/cm/Torr. Figure 1 compares the results.

After the evaluation of A and B, general expression for the electric field is obtained from Poisson's equation in the absence of space charge: $\nabla^2 V = 0$ with the following boundary conditions:

$$E(c) = \delta E_0 \qquad V(R_2) = 0 \tag{3}$$

where V is the electric potential ($E = -\vec{\nabla} V$), R_2 is an arbitrarily large distance from the electrode where the voltage is 0 and c is the position of the corona front. The ratio $\delta = \frac{p}{p_0}$ is a scaling factor for different pressures, and E_0 is the classic breakdown electric field. Beyond the corona front ($r > c$), E falls below the classic breakdown electric field, causing ionization to stop, and yielding the first boundary condition. We then substitute E in (1) and solve for c. Finally an expression for the critical voltage is obtained as a function of d for corona discharge in Cartesian geometry and R_1 and R_2 as $V_\mathrm{c} = V(R_1)$, for corona discharge around cylindrical or spherical objects.

CARTESIAN COORDINATES

Townsend discharge in the Cartesian case involves two parallel plates, some distance d apart with a gas at a pressure, p. Townsend's equation (2) approximates the experimental data well, though the model fails at higher values of pd (pressure·distance) in part because of the appearance of different ionization phenomena such as the formation of streamers, which require a different model.[9, 19]

The Cartesian solution of Townsend's breakdown is well-known and studied by various authors.[3, 4] Due to symmetry, the electric field is uniform between the two

§The air1.m function can also be used, though slightly different values of A and B will be acquired. The air1.m function is explained in detail in [28] and can be found at pasko.ee.psu.edu/air/air1.m. For the purposes of this paper, only formulations of Morrow and Lowke[27] employed.

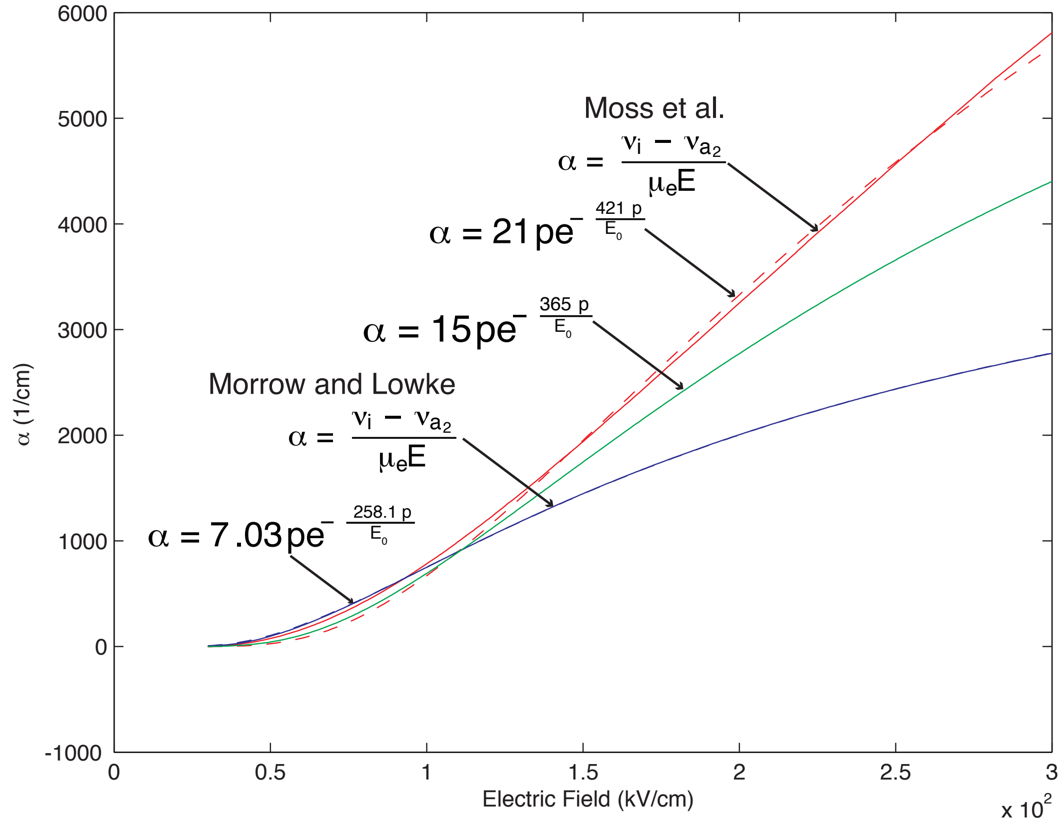

..

Figure 1: The values of α for different models

plates which simplifies the integral of equation (1). Substituting Equation (2) into Equation (1), gives:

$$\int_{R_1}^{R_2} \left(Ape^{-\frac{Bp}{E}}\right) dr = \left(Ape^{-\frac{Bp}{E}}\right) \int_{R_1}^{R_2} dr = Ap\underbrace{(R_2 - R_1)}_{d}e^{-\frac{Bp}{E}} = \ln Q \quad (4)$$

Solving equation (4) for E and noting that $V = Ed$ due to the uniform electric field gives:

$$E = -\frac{Bp}{\ln\left(\frac{\ln Q}{Apd}\right)} \;; \qquad V = -\frac{Bpd}{\ln\left(\frac{\ln Q}{Apd}\right)} \quad (5)$$

This well-known result can be found in [3, 4] under the form: $V = \frac{Bpd}{\ln(pd)+\ln\left(\frac{A}{\ln Q}\right)}$. Stoletov's minimum values are obtained as:[3]

$$d_{\min} = \frac{e}{Ap}\ln Q \;; \qquad E_{\min} = Bp \;; \qquad V_{\min} = \frac{eB}{A}\ln Q \quad (6)$$

CYLINDRICAL COORDINATES

In this section, we calculate the critical breakdown voltage in a cylindrical geometry as a function of the radii R_1 and R_2 of the inner and outer electrodes. The derived equations will be in terms of R_1 and R_2 as opposed to d since it is well established that ionization is a function of the breakdown electric field (E_0) and the curvature radius (R_1) of the electrode.[29] The cylindrical case starts off with Poisson's equation in cylindrical coordinates (r, ϕ, z). Assuming symmetry with respect to ϕ and z, we have $\frac{\partial V}{\partial \phi} = 0 = \frac{\partial V}{\partial z}$. Poisson's equation for an axisymmetric cylindrical geometry with no axial variation gives:[4] $\frac{1}{r}\frac{\partial}{\partial r}\left(r\frac{\partial V}{\partial r}\right) = 0$. The solution of this differential equation is:

$$V = k_1 \ln r + k_2 \tag{7}$$

where k_1 and k_2 are integration constants. Using the boundary conditions specified by (3), we have $E(c) = \delta E_0$, for which ionization equals attachment.[11] Additionally, the voltage will be zero at a distance R_2 that is sufficiently larger than R_1. In this work, we used $R_2 = 1$ m. Using these boundary conditions, the equations for voltage and electric field can be found as:

$$E = \frac{\delta E_0 c}{r} \quad ; \qquad V = \delta E_0 c \ln \frac{R_2}{r} \tag{8}$$

Substituting (8) into Equation (1), we obtain:

$$\int_{R_1}^{c} Ape^{-\frac{Bp}{E}} = \int_{R_1}^{c} Ape^{-\frac{Bpr}{\delta E_0 c}} = \frac{Apc\left(e^{-\frac{Bp}{\delta E_0}} - e^{-\frac{BpR_1}{\delta E_0 c}}\right)}{-\frac{Bp}{\delta E_0}} = \ln Q \tag{9}$$

which we solve for c. An analytical approximation of the solution can be obtained through a Taylor expansion of the exponential term, $e^{-\frac{BpR_1}{\delta E_0 c}} \approx 1 - \frac{BpR_1}{\delta E_0 c}$. This is justified by noting that in reality, $c \gg R_1$.[11] Substituting into Equation (9) and simplifying yields a closed form solution for c, $c = B\left(\ln Q + ApR_1\right) / \left(A\delta E_0\left(1 - e^{\frac{-Bp}{\delta E_0}}\right)\right)$. Having substituted c into Equation (8) leads to:

$$V(r) = \frac{B\ln\left(\frac{R_2}{r}\right)(\ln Q + ApR_1)}{A(1 - e^{\frac{-Bp}{\delta E_0}})} \quad E(r) = \frac{B(\ln Q + ApR_1)}{rA(1 - e^{\frac{-Bp}{\delta E_0}})} \tag{10}$$

and consequently,

$$V_{\mathrm{c}} = V(R_1) = \frac{B\ln\frac{R_2}{R_1}(\ln Q + ApR_1)}{A(1 - e^{-\frac{Bp}{\delta E_0}})} \, ; \, E_{\mathrm{c}} = E(R_1) = \frac{B(\ln Q + ApR_1)}{AR_1(1 - e^{-\frac{Bp}{\delta E_0}})} \tag{11}$$

The minimum of V_c with respect to R_1 occurs at the root, $R_{\min}$ of $\frac{\partial V_c}{\partial R_1} = 0$. Solving for R_1 gives:

$$R_1 = R_{\min} = \frac{-\ln Q}{Ap \cdot \mathrm{ProductLog}\left(\frac{e \ln Q}{ApR_2}\right)} \tag{12}$$

where ProductLog is the inverse function of $f(x)$=xe^x. In order to obtain a simpler form of (12), a first order Taylor expansion is used, $\mathrm{ProductLog}(-x) \approx -j\pi + \ln(-x)$[§]. This leads to:

$$R_{\min} = -\frac{\ln Q}{Ap\left(j\pi + \ln\left(\frac{-e \ln Q}{ApR_2}\right)\right)}$$

Since $\ln(-e) = j\pi + 1$, the imaginary part of the solution cancels leaving a purely real answer of:

$$R_{\min} = \frac{-\ln Q}{Ap\left(1 + \ln \frac{\ln Q}{ApR_2}\right)} \tag{13}$$

The minimum critical electric field and voltage can be found by substituting Equation (13) into (11):

$$\left\{\begin{array}{rcl} \lambda & = & \frac{\ln Q}{ApR_2} \\ \kappa & = & \frac{Bp_0}{E_0} \\ V_{\min} & = & \dfrac{B}{A}\dfrac{\ln Q}{1 + 1/\ln\lambda}\dfrac{\ln\left(-\frac{1}{\lambda}\left(1 + \ln\lambda\right)\right)}{1 - \exp(-\kappa)} \\ E_{\min} & = & \dfrac{Bp\ln\lambda}{\exp(\kappa) - 1} \end{array}\right. \tag{14}$$

SPHERICAL COORDINATES

Deriving the minimum breakdown voltage for corona discharge in spherical coordinates uses the same assumptions as those employed in the cylindrical case. We start with Poisson's equation in spherical coordinates (r, θ, ϕ). The electric field is now independent of θ and ϕ, as opposed to ϕ and z. In spherical coordinates, the general solution for the electric potential becomes:

$$V = -\frac{k_1}{r} + k_2$$

[§]In certain intervals, ProductLog has more than one solution. For sake of continuity, the principal root is generally used, but in this particular application, the correct root was not the principal root (the principal root will give a solution that breaks the assumption that $R_2 \gg R_1$). The Taylor expansion used converges to the desired root as opposed to the principal root. ProductLog is also known as the Lambert-W or Omega function. For more information on the ProductLog function, visit http://documents.wolfram.com/mathematica/functions/ProductLog.

Using the boundary conditions (3), we obtain formulas for potential and electric field.

$$V(r) = c^2\delta E_0\left(\frac{1}{r} - \frac{1}{R_2}\right) \quad ; \qquad E(r) = \frac{c^2\delta E_0}{r^2} \tag{15}$$

The value of c is obtained from substituting (15) into Equation (1), which yields the following integral:

$$\int_{R_1}^{c} Ape^{\frac{-Bpr^2}{\delta E_0 c^2}}\, dr = \ln Q$$
$$\frac{Apc\sqrt{\pi}\sqrt{\delta E_0}}{2\sqrt{Bp}}\left(\text{Erf}\left(\sqrt{\frac{Bp}{\delta E_0}}\right) - \text{Erf}\left(\frac{R_1}{c}\sqrt{\frac{Bp}{\delta E_0}}\right)\right) = \ln Q \tag{16}$$

where $\text{Erf}(x) = \frac{2}{\sqrt{\pi}}\int_0^x e^{-t^2}\, dt$. As previously, we use a Taylor expansion: $\text{Erf}(x) \approx \frac{2x}{\sqrt{\pi}}$. This approximation is justified by noting that $c \gg R_1$ (and therefore $\frac{R_1}{c} \approx 0$). For typical values ($B \simeq 258$ V/cm/Torr, $E_0 \simeq 31$ kV/cm, $\delta = 1$, and $p = 760$ Torr), $\text{Erf}\left(\sqrt{\frac{Bp}{\delta E_0}}\right) \approx 1$. This leads to:

$$\text{Erf}\left(\sqrt{\frac{Bp}{\delta E_0}}\right) \approx 1 \quad ; \qquad \text{Erf}\left(\frac{R_1}{c}\sqrt{\frac{Bp}{\delta E_0}}\right) \approx \frac{2}{\sqrt{\pi}}\frac{R_1}{c}\sqrt{\frac{Bp}{\delta E_0}} \tag{17}$$

Substituting Equation (17) into Equation (16) gives, after simplification $c = \frac{2\sqrt{Bp}}{Ap\sqrt{\pi\delta E_0}}$, which with (15) gives:

$$V(r) = \frac{4B\left(\ln Q + ApR_1\right)^2}{\pi A^2 p}\left(\frac{1}{r} - \frac{1}{R_2}\right) E(r) = \frac{4B\left(\ln Q + ApR_1\right)^2}{\pi A^2 p r^2} \tag{18}$$

Although imperfect, the above approximation provides a practical analytical solution for the voltage needed to initiate a corona discharge around spherical objects. Since the critical voltage and electric field will occur at the inner electrode, the critical voltage is:

$$\begin{aligned} V_{\text{c}} &= V(R_1) = & \frac{4B\left(\ln Q + ApR_1\right)^2}{\pi A^2 p}\left(\frac{1}{R_1} - \frac{1}{R_2}\right) \\ E_{\text{c}} &= E(R_1) = & \frac{4B\left(\ln Q + ApR_1\right)^2}{\pi A^2 p R_1^2} \end{aligned} \tag{19}$$

The minimum voltage for corona breakdown is obtained by solving $\frac{\partial V_{\text{c}}}{\partial R_1} = 0$. Solving for R_1 results in a cubic equation with three roots:

$$R_1 = -\frac{\ln Q}{Ap} \quad ; \qquad R_1 = \frac{R_2}{4}\left(1 \pm \sqrt{1 - \frac{8\ln Q}{ApR_2}}\right) \tag{20}$$

The first root is extraneous (R_1 cannot be negative), and the second root is forbidden by the assumption that $R_2 \gg R_1$. This leaves the third root which is:

$$R_1 = R_{\min} = \frac{R_2}{4}\left(1 - \sqrt{1 - \frac{8\ln Q}{ApR_2}}\right) \tag{21}$$

In reality, we have $R_2 \to \infty$. This limit diverges in cylindrical geometry due to the logarithm, but in spherical coordinates, we get:

$$R_{\min} = \lim_{R_2\to\infty} \frac{R_2}{4}\left(1 - \sqrt{1 - \frac{8\ln Q}{ApR_2}}\right) = \frac{\ln Q}{Ap} \tag{22}$$

Assuming R_2 is infinite and substituting (22) into (19), the critical electric field and voltage in spherical coordinates are:

$$E_{\min} = \frac{16Bp}{\pi} \quad ; \qquad V_{\min} = \frac{16B\ln Q}{\pi A} \tag{23}$$

RESULTS

Using the revised values of A and B fitted using Morrow and Lowke's[27] values for ν_i, ν_{a_2}, and μ_e, the obtained analytical solutions are in good agreement with the numerical solution for all three geometries, most notably around the minimum. The values at the minimum for both cylindrical and spherical geometries are shown in Table II.

Table II: Critical Values in Cylindrical and Spherical geometry.

Parameter	Numerical	Analytical	% Error
	Cylindrical		
Critical Radius (cm)	1.4×10^{-4}	1.5×10^{-4}	8%
Critical Electric field (kV/cm)	3.3×10^{4}	3.6×10^{4}	9%
Critical Voltage (kV)	4.9	4.9	0.6%
	Spherical		
Critical Radius (cm)	2.3×10^{-3}	1.7×10^{-3}	26%
Critical Electric field (kV/cm)	2.6×10^{3}	1.0×10^{3}	61%
Critical Voltage (kV)	6.0	1.7	71%

Figure 2(a) plots the breakdown voltage V_c (V) for each geometry as a function of the product, pd or pR_1 (cm-Torr) in the same way as the original Paschen curve. Solid lines indicate the analytical solutions and dashed lines indicate the numerical solution using Morrow and Lowke's[27] models. Arrows point to both the numerical and analytical solutions in Cartesian, cylindrical, and spherical geometries. Also, (car.) indicates the Cartesian solution, (cyl.) indicates the cylindrical solutions, and (sph.) indicates the spherical solutions. An '$\times$' denotes the location of the minimum on each curve.

Figure 2(b) plots the breakdown voltage V_c (V) for each geometry as a function of δd or δR_1 (m). As in Figure 2(a), solid lines indicate analytical solutions, dashed lines indicate the numerical models based on Morrow and Lowke's[27] models and (car.), (cyl.), and (sph.) correspond to Cartesian, cylindrical, and spherical geometries, respectively. The minima are also marked with '$\times$'. The axes were scaled to show the location of the minimum in cylindrical geometries, which occurs towards the left side of the graph.

Figure 2(c) plots the breakdown electric field E_c (V/m) as a function of δd or δR_1 (m) for each geometry with the same legend as the two prior graphs. Here, '$\times$' denotes the location of $R_{\min}$ and the critical electric field for this value.

Finally, Figure 3 compares breakdown voltage (V) as a function of δR_1 (m) for the models of cylindrical and spherical onset corona proposed by Lowke and D'Alessandro[11] to the analytical and numerical voltages obtained in the previous section, in cylindrical and spherical geometry, respectively. The arrows point to the numerical solution, the analytical solution, and the curve corresponding to the models of Lowke and D'Alessandro.[11] As previously, an '$\times$' is placed at the minimum where applicable.

DISCUSSION AND COMPARISON

In this section, we discuss the significance and accuracy of the numerical and analytical solutions to the problem of breakdown voltage for initiation of Townsend discharge in a parallel plate configuration and of corona discharges in cylindrical and spherical geometries. The curves of the Cartesian solution in Figure 2(a) represent the classic solution to the Cartesian problem, and show the well-known form of the Paschen curves [e.g., 3]. For large values of δR_1, the numerical solutions of all geometries converge toward the cartesian solution, since both cylindrical and spherical geometries will locally behave like a plane-plane configuration when the two electrodes are closer together.

Paschen curves show that the critical electric field is dependent on the product pd, i.e., the corona breakdown voltage follows a similarity law.[3, 29] In the case of the spherical analytical solution, the voltage is a function of the product: pR_1. These results, namely that the breakdown voltage follows a similarity law, suggest that initiation of a corona around a spherical object can be minimized for a given radius by modifying the pressure. In the atmosphere, this could be accomplished by lifting the object to higher altitudes, i.e. to lower pressures. The critical radius, electric field, and breakdown voltage in spherical geometry has a nearly identical form to the values at Stoletov's point in Cartesian geometry, the difference being

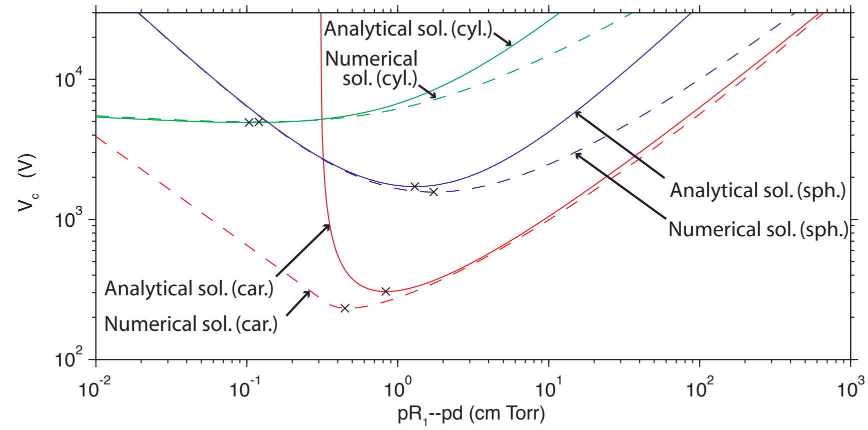

(a) Comparison of the breakdown voltages with respect to pd or pR_1. The dashed lines show the numerical solutions, while solid lines show the analytical solutions. The (car.), (cyl.), and (sph.) additions correspond to the Cartesian, cylindrical, and spherical solutions respectively.

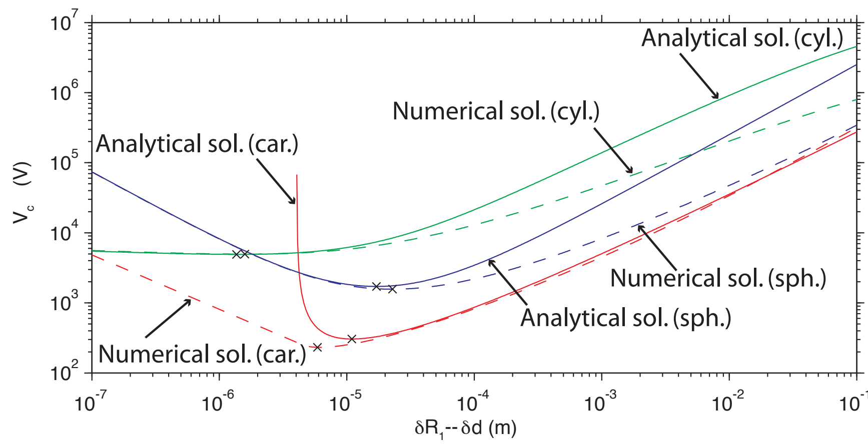

(b) Comparison of the breakdown voltages with respect to δd or δR_1. The legend is the same as in part (a).

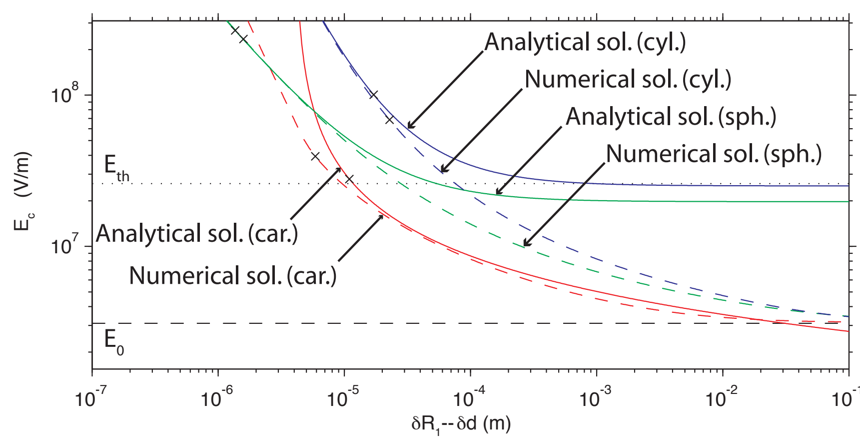

(c) Comparison of the critical electric fields. The legend is the same as in part(a) and (b).

Figure 2: Comparison of numerical and analytical solutions.

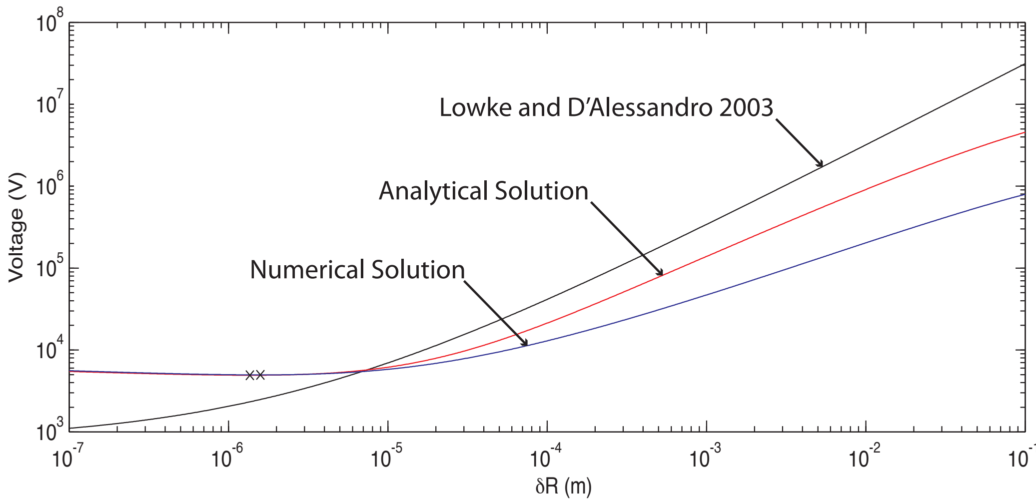

..

(a) Comparison of breakdown voltage curves in the cylindrical case. The top two curves correspond to the analytical and numerical solutions respectively. The bottom curve represents Lowke and D'Alessandro's[11] solution.

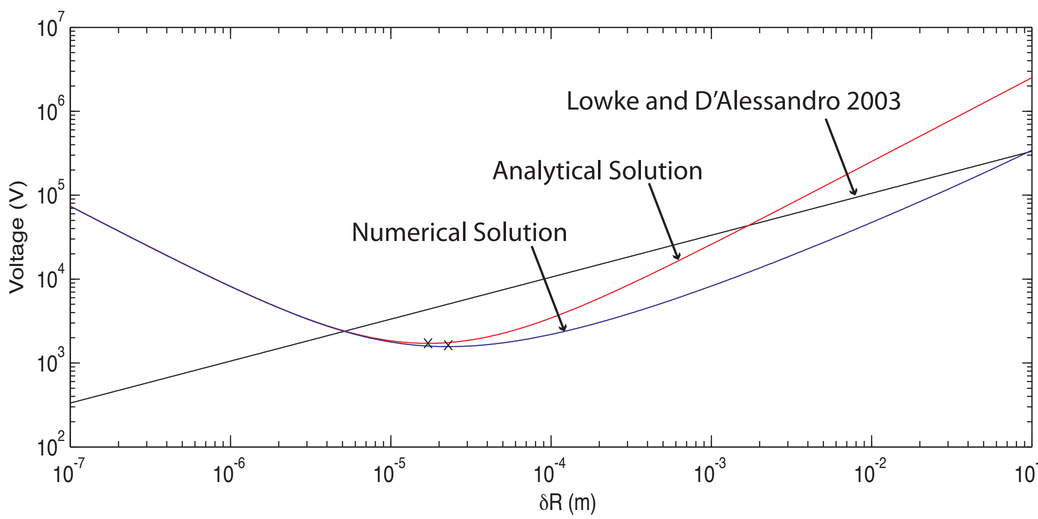

..

(b) Same as plot (a) only for a spherical geometry.

Figure 3: Breakdown curves in various geometries.

a factor of $\frac{16}{\pi}$ as opposed to e, i.e, a factor of $\sim$2 (1.87). It appears that cylindrical geometries do not follow the same similarity law due to the presence of a logarithm in the analytical solution.

While Gary *et al.*[19] states that Townsend's equation is "satisfactory" for higher values of E, the cylindrical and spherical case diverge from the numerical solutions at these values. A possible explanation to this observation lies in the assumption that $\frac{R_1}{c} \approx 0$ in the Taylor expansion of the ProductLog and Erf functions. In reality, it is possible that $c \not\gg R_1$ which may limit the accuracy of the analytical formulas.

Lowke and D'Alessandro[11] use a quadratic model in the cylindrical case and a linear model in the spherical case due to the difficulty in solving these expressions analytically. Figure 3 shows that Lowke and D'Alessandro's[11] models are roughly an order of magnitude different from either the numerical or analytical solution in both geometries. The fit could be improved if numerical parameters in Lowke and D'Alessandro's formulas were adjusted in a similar way to that used in this work for the coefficients of A and B.

In spherical geometry, Lowke and D'Alessandro's[11] model for voltage differs by several orders of magnitude for low values of δR_1, but agreement is reasonable near the minimum $\delta R_1 \approx 2 \times 10^{-5} = 20\ \mu$m. This complements the analytical solution which is more accurate for lower values δR_1, but the linear approximation is overall less accurate than the Townsend equation in spherical geometry. Additionally, Lowke and D'Alessandro's model does not show a minimum point which is suggested by the results of our work.

It should be noted that the minima obtained in this study using Townsend's equation in Cartesian, cylindrical, and spherical geometries appeared to be associated with critical electric fields that exceed the thermal runaway electric fields ($E_{\text{th}} \approx 260$ kV/cm[28]). This suggests that classic estimates of Stoletov's point in Paschen theory as well as the new results presented in this study, should be regarded cautiously as they may be located in a region where ionization and two-body attachment could not be the dominant processes. In addition, theoretical minimum radii are on the order of μm, corresponding to very small or very sharp pointed lightning rods, which does not explain at present the results of the field studies by Moore *et al.*.[1, 2, 24] Consequently, further research is required to determine the lightning rod optimum radius and to give an accurate theoretical explanation for Moore *et al.*'s results.

CONCLUSIONS

Corona onset is fundamental for creation of an upward leader[21] and hence for the development of more effective lightning rods.[11] Golde[20, 21] hypothesized that the lightning rod's efficiency is dependent on how readily upward leaders form from the lightning rod's tip; however, Golde's hypothesis has not yet been confirmed theoretically.[7] Moore *et al.*'s experiments suggest that there is an optimum radius, but none of the published models based on Peek's equation allow for the evaluation of a minimum.[11, 19] The models presented in this paper introduce analytical formulas as well as numerical solutions, that allow for a first estimation of the critical radius and minimum breakdown voltage for corona discharge around lightning rods in cylindrical and spherical geometries. However, these models predict electric fields that exceed thermal runaway of the electric field for corona onset (≈ 260 kV/cm).[28] To resolve this issue, proposed models may be further improved by fitting the constants A and B not only to different proposed numerical models, but by restricting the fits to more realistic electric fields for corona discharge. Additionally, other factors such as space charge effects need to be considered as well in theoretical models of upward leader development.[22]

ACKNOWLEDGEMENT

This material is based upon work supported by the National Science Foundation under Grant, No. EEC-0755081 and ATM-0652148.

REFERENCES

1 C. B. Moore, G. D. Aulich and W. Rison, "Measurements of lighting rod responses to nearby strikes," *Geophys. Res. Lett.*, **27** (10) 1487–1490 (2000b).

2 C. B. Moore, W. Rison, J. Mathis and G. Aulich, "Lightning rod improvement studies," *J. Appl. Meteor.*, **39** (5) 593–609 (2000a).

3 Y. P. Raizer, *Gas Discharge Physics*, Springer-Verlag, New York, NY, 1991.

4 R. J. Roth, *Industrial plasma engineering, Vol. 1: Principles*, IOP Publishing Ltd, 1995.

5 V. A. Rakov and M. A. Uman, *Lightning: Physics and Effects*, Cambridge Univ. Press, Cambridge, U.K.; New York, 2003.

6 N. L. Aleksandrov, E. M. Bazelyan, F. D'Alessandro and Y. P. Raizer, "Dependence of lightning rod efficacy on its geometric dimensions–a computer simulation," *J. Phys. D: Appl. Phys.*, **38** (1) 1225–1238, doi:10.1088/0022-377/38/8/021 (2005).

7 N. L. Aleksandrov, E. M. Bazelyan and Y. P. Raizer, "The effect of a corona discharge on a lightning attachment," *Plasma Phys. Rep.*, **31** (1) 75–91 (2005).

8 N. Y. Liu and V. P. Pasko, "Effects of Photoionization on Similarity Properties of Streamers at Various Pressures in Air," *J. Phys. D: Appl. Phys.*, **39** 327–334, doi:10.1088/0022-3727/39/2/013 (2006).

9 E. M. Bazelyan and Y. P. Raizer, *Spark Discharge*, Chemical Rubber Company Press, New York, NY, 1998.

[10] N. L. Aleksandrov, E. M. Bazelyan, F. D'Alessandro and Y. P. Raizer, "Numerical simulations of thunderstorm-induced corona processes near lightning rods installed on grounded structures," *J. Electrostat.*, **64** (12) 802–816, doi: 10.1016/j.elstat.2006.02.001 (2006).

[11] J. J. Lowke and F. D'Alessandro, "Onset corona fields and electrical breakdown criteria," *J. Phys. D: Appl. Phys.*, **36** (21) 2673–2682, doi:10.1088/0022-3727/36/21/013 (2003).

[12] N. L. Aleksandrov, A. E. Bazelyan, E. M. Bazelyan and I. V. Kochetov, "Modeling of Long Streamers in Atmospheric-Pressure Air," *Plasma Phys. Rep.*, **21** (60) 57–75 (1995).

[13] N. Aleksandrov, E. Bazelyan and A. Konchakov, "Plasma parameters in the channel of a long leader in air," *Plasma Physics Reports*, **27** (10) 875–885 (2001).

[14] J. A. Riousset, *Fractal modeling of lightning discharges*, Master's thesis, The Pennsylvania State University, University Park, PA (2006).

[15] I. Gallimberti, G. Bacchiega, A. Bondiou-Clergerie and P. Lalande, "Fundamental processes in long air gap discharges," *C. R. Physique*, **3** (10) 1335–1359, doi:10.1016/S1631-0705(02)01414-7 (2002).

[16] N. A. Popov, "Formation and development of a leader channel in air," *Plasma Phys. Rep.*, **29** (8) 695–708, doi:10.1134/1.1601648 (2003).

[17] E. M. Bazelyan and Y. P. Raizer, *Lightning Physics and Lightning Protection*, IoP Publishing Ltd, Bristol, UK and Philadelphia, PA, 2000.

[18] A. V. Gurevich, K. P. Zybin and Y. V. Medvedev, "Runaway breakdown in strong electric field as a source of terrestrial gamma flashes and gamma bursts in lightning leader steps," *Phys. Lett. A.*, **361** 119–125, doi: 10.1016/j.physleta.2006.05.063 (2007).

[19] C. Gary, J. Schmitt and B. Hutzler, "Peeks Law Generalization Application To Various Field Configurations," *IEEE Transactions On Power Apparatus and Systems*, **PA91** (6) 2262–& (1972).

[20] R. H. Golde, ed., *Lightning*, vol. 1: Physics of Lightning, Academic Press, London, UK; New York, NY, 1977.

[21] R. H. Golde, ed., *Lightning*, vol. 2: Lightning Protection, Academic Press, London, UK; New York, NY, 1977.

[22] F. D'Alessandro and G. Berger, "Laboratory studies of corona emissions from air terminals," *Journal of Physics D-Appied Physics*, **32** (21) 2785–2790 (1999).

[23] R. H. Golde, “Lightning Conductor,” *Journal of the Franklin Institute-Engineering and Applied Mathematics*, **283** (6) 451–& (1967).

[24] C. B. Moore, G. D. Aulich and W. Rison, “The case for using blunt-tipped lightning rods as strike receptors,” *J. Appl. Meteor.*, **42** (7) 984–993 (2003).

[25] F. D’Alessandro, “On the optimum rod geometry for practical lightning protection systems,” *J. Electrostat.*, **65** (2) 113–121, doi:10.1016/j.elstat.2006.07.011 (2007).

[26] F. D’Alessandro and J. Gumley, “A “Collection Volume Method” for the placement of air terminals for the protection of structures against lightning,” *Journal of Electrostatics*, **50** (4) 279–302 (2001).

[27] R. Morrow and J. J. Lowke, “Streamer propagation in air,” *J. Phys. D: Appl. Phys.*, **30** 614–627 (1997).

[28] G. D. Moss, V. P. Pasko, N. Liu and G. Veronis, “Monte Carlo model for analysis of thermal runaway electrons in streamer tips in transient luminous events and streamer zones of lightning leaders,” *J. Geophys. Res.*, **111** A02307, doi: 10.1029/2005JA011350 (2006).

[29] N. Spyrou, R. Peyrous, N. Soulem and B. Held, “Why Paschens Law Does Not Apply in Low-Pressure Gas-Discharges With Inhomogeneous Fields,” *Journal of Physics D-Appied Physics*, **28** (4) 701–710 (1995).